

generated February 5, 2018

The abundance of C_3H_2 and other small hydrocarbons in the diffuse interstellar medium ¹

Harvey Liszt

*National Radio Astronomy Observatory
520 Edgemont Road, Charlottesville, VA 22903-2475*

and

Paule Sonnentrucker

*Space Telescope Science Institute
3700 San Martin Dr, Baltimore, MD 21218*

and

Martin Cordiner

*Astrochemistry Laboratory and the Goddard Center for Astrobiology
Mailstop 691, NASA Goddard Space Flight Center
8800 Greenbelt Road, Greenbelt, MD 20770, USA*

and

Maryvonne Gerin

*LERMA, UMR 8112 du CNRS, Observatoire de Paris
École Normale Supérieure, UPMC & UCP, France*

hliszt@nrao.edu

ABSTRACT

Hydrocarbons are ubiquitous in the interstellar medium, observed in diverse environments ranging from diffuse to molecular dark clouds and strong photon-dominated regions near HII regions. Recently, two broad diffuse interstellar bands (DIBs) at 4881Å and 5450Å were attributed to the linear version of propynylidene $l-C_3H_2$, a species whose more stable cyclic conformer $c-C_3H_2$ has been widely observed in the

diffuse interstellar medium at radio wavelengths. This attribution has already been criticized on the basis of indirect plausibility arguments because the required column densities are quite large, $N(l\text{-C}_3\text{H}_2)/E_{\text{B-V}} = 4 \times 10^{14} \text{ cm}^{-2} \text{ mag}^{-1}$. Here we present new measurements of $N(l\text{-C}_3\text{H}_2)$ based on simultaneous 18-21 GHz VLA absorption profiles of cyclic and linear C_3H_2 taken along sightlines toward extragalactic radiocontinuum background sources with foreground Galactic reddening $E_{\text{B-V}} = 0.1 - 1.6 \text{ mag}$. We find that $N(l\text{-C}_3\text{H}_2)/N(c\text{-C}_3\text{H}_2) \approx 1/15 - 1/40$ and $N(l\text{-C}_3\text{H}_2)/E_{\text{B-V}} \approx 2 \pm 1 \times 10^{11} \text{ cm}^{-2} \text{ mag}^{-1}$, so that the column densities of $l\text{-C}_3\text{H}_2$ needed to explain the diffuse interstellar bands are some three orders of magnitude higher than what is observed. We also find $N(\text{C}_4\text{H})/E_{\text{B-V}} < 1.3 \times 10^{13} \text{ cm}^{-2} \text{ mag}^{-1}$ and $N(\text{C}_4\text{H}^-)/E_{\text{B-V}} < 1 \times 10^{11} \text{ cm}^{-2} \text{ mag}^{-1}$ (3σ). Using available data for CH and C_2H we compare the abundances of small hydrocarbons in diffuse and dark clouds as a guide to their ability to contribute as DIB carriers over a wide range of conditions in the interstellar medium.

Subject headings: astrochemistry . ISM: molecules . ISM: clouds. Galaxy

1. Introduction

The cyclic (ring) conformer of propynylidene, $c\text{-C}_3\text{H}_2$, was discovered and identified in the interstellar medium (ISM) by Matthews & Irvine (1985) and Thaddeus et al. (1985) and quickly recognized as a ubiquitous tracer of molecular gas in both dark (Madden et al. 1989; Cox et al. 1989) and diffuse clouds (Cox et al. 1988). It is abundant even in strong photon-dominated regions (PDR) like the Horsehead Nebula (Pety et al. 2005). Extensive recent surveys of the small hydrocarbons $c\text{-C}_3\text{H}_2$ and C_2H in mm-wave absorption (Lucas & Liszt 2000a; Gerin et al. 2011) show that they have a nearly-fixed relative abundance $N(\text{C}_2\text{H})/N(c\text{-C}_3\text{H}_2) \approx 20$ in diffuse gas, much above that seen in the dark cloud TMC-1 where $N(\text{C}_2\text{H})/N(c\text{-C}_3\text{H}_2) \approx 2$ (Ohishi et al. 1992), and a nearly constant abundance with respect to H_2 , $X(c\text{-C}_3\text{H}_2) = N(c\text{-C}_3\text{H}_2)/N(\text{H}_2) \approx 2 - 3 \times 10^{-9}$.

By contrast, when the less stable linear conformer $l\text{-C}_3\text{H}_2$ was detected in the ISM (Cernicharo et al. 1991) it was found to be much less abundant than $c\text{-C}_3\text{H}_2$ in the dark cloud TMC1, with $N(c\text{-C}_3\text{H}_2)/N(l\text{-C}_3\text{H}_2) \approx 100$ and $N(l\text{-C}_3\text{H}_2) = 2.5 \times 10^{12} \text{ cm}^{-2}$. Subsequent observations of $l\text{-C}_3\text{H}_2$ in mm-wave absorption from diffuse clouds in front of the distant HII regions W49 and W51 (Cernicharo et al. 1999) found that the ratio $c\text{-C}_3\text{H}_2/l\text{-C}_3\text{H}_2$ was smaller, $N(c\text{-C}_3\text{H}_2)/N(l\text{-C}_3\text{H}_2) = 3\text{-}7$, although with small column densities overall, $N(l\text{-C}_3\text{H}_2) \lesssim 5 \times 10^{11} \text{ cm}^{-2}$.

¹Based on observations obtained with the NRAO Jansky Very Large Array (VLA).

Despite strong suggestions that column densities of $l\text{-C}_3\text{H}_2$ are modest in the ISM, whether in diffuse or dark gas, Maier et al. (2011b) recently hypothesized that broad diffuse interstellar bands (DIBs) at 4881\AA and 5450\AA are produced by a ground-state electronic transition of $l\text{-C}_3\text{H}_2$, with $N(l\text{-C}_3\text{H}_2) \approx 2 - 5 \times 10^{14}$ toward HD 206267 ($E_{B-V} = 0.52$ mag) and HD 183143 ($E_{B-V} = 1.27$ mag). This assignment has already been criticized for obvious reasons based on indirect plausibility arguments (Krełowski et al. 2011; Oka & McCall 2011). Here we show directly that the diffuse ISM is in no way anomalous with regard to the $l\text{-C}_3\text{H}_2$ abundance. Seen in absorption originating in Galactic diffuse and translucent clouds occulting 4 compact extragalactic mm-wave continuum sources along sightlines with $E_{B-V} = 0.1$ mag - 1.6 mag, column densities of $l\text{-C}_3\text{H}_2$ are indeed small, with $N(l\text{-C}_3\text{H}_2) \lesssim 1 - 3 \times 10^{11} \text{ cm}^{-2}$.

The plan of this work is as follows. In Section 2 we describe new 18-21 GHz absorption line observations of $l\text{-C}_3\text{H}_2$, $c\text{-C}_3\text{H}_2$, C_4H and C_4H^- . In Section 3 we discuss the abundances and column densities of these and other small hydrocarbons so that their ability to contribute as carriers of DIBs may be accurately assessed.

2. Observations, conventions and conversion from optical depth to column density

The new observations reported here were taken at the National Radio Observatory’s Jansky Very Large Array (VLA) on 16 and 17 September 2011 under proposals 11B/003 (for C_3H_2) and 11B/076 (for C_4H and its anion C_4H^-), in “move” time during the A-D configuration transition. The data were taken in four schedule blocks (SB) of 2 hour duration observing in two orthogonal polarizations in each of two basebands with all of the 4 basebands covered by 6 contiguous spectral windows having 128 independent channels over a bandwidth 2 MHz. The spectral lines observed here, all in the range 18-21 GHz, are summarized in Table 1. At 20 GHz, a bandwidth of 2 MHz corresponds to 30 km s^{-1} so that the widths of the spectral line channels were all approximately $30 \text{ km s}^{-1}/128 \approx 0.25 \text{ km s}^{-1}$. All velocities discussed here are relative to the kinematic definition of the Local Standard of Rest that is in universal use at radio telescopes.

Properties of the sources and sightlines observed and their integrated molecular optical depths are summarized in Table 2; two targets and a bandpass calibrator (3C84) were covered in each SB. Considerable time was devoted to reference pointing on each continuum source before it was observed. No absolute amplitude calibration was performed but the fluxes relative to that of the bandpass calibrator ($S_\nu \approx 16 \text{ Jy}$) are given in Table 2. In each SB the bandpass calibrator was observed for approximately 20m. B2251+158 was observed for approximately 18 minutes and the other sources for approximately 40m during any one SB. The weather and system temperatures were significantly better during the observing for 11B/003 ($l\text{-C}_3\text{H}_2$ and $c\text{-C}_3\text{H}_2$) as reflected in the rms noise levels reported in Table 2. As well, some unexplained malfunction resulted in loss of

much of the flux during the search for C_4H toward 3C111, as reflected in Table 2 and beyond.

The data were reduced using very standard techniques in CASA. The bandpass calibrator observations were phase-calibrated during each scan sub-interval followed by construction of an average bandpass solution. This was applied on the fly to complex gain-cal solutions for each continuum target at the sub-scan level, followed by scan-length gain calibration solutions that were applied to each target individually. Once the data were passband and phase-calibrated in this way they were also fully reduced within CASA owing to the point-like nature of the background targets. For each polarization and baseband the final spectra were extracted as the vector phase average over all visibilities, without gridding or mapping the data. The vector average spectra were produced in CASA’s plotms visualizer for uv-visibilitys and exported to standard singledish software where the polarizations were co-added and very small linear baselines amounting typically to 0.01% of the continuum were removed from end to end across each of the basebands.

The optical depth-column density conversion factors in Table 1 were computed assuming rotational excitation in equilibrium with the cosmic microwave background. The validity of this assumption is verified by the excellent agreement between column densities of $c-C_3H_2$ derived here and previously by Lucas & Liszt (2000a) from observations of a higher-frequency transition arising out of the same lower level (see Table 3). Note that only one spin-ladder of either version of C_3H_2 was actually observed here, ortho- $c-C_3H_2$ and para- $l-C_3H_2$, and the tabulated conversion factors apply only to the ortho or para version that was observed. Nominally, the ortho:para ratio is 3:1 in either species so that $N(c-C_3H_2) = 4/3 N(o-c-C_3H_2)$, $N(l-C_3H_2) = 4 N(p-l-C_3H_2)$ and $N(l-C_3H_2)/N(c-C_3H_2) = 3 N(p-l-C_3H_2)/N(o-c-C_3H_2)$. 3:1 ortho:para ratios are used to convert from specific to total molecular column density in Tables 3 and 4. The mean $o-c-C_3H_2/p-c-C_3H_2$ ratio measured by Lucas & Liszt (2000a) in three directions (including B0355 and B0415) was 3.0, with considerable scatter.

Table 3 gives total molecular column densities per unit reddening using the integrated optical depths shown in Table 2 and 3:1 ortho:para ratios, and Table 4 compares fractional abundances in diffuse clouds with those toward TMC-1, using mean quantities and upper limits from Table 3 for the diffuse gas and various results taken from the literature including $N(H_2) = 1 \times 10^{22} H_2 \text{ cm}^{-2}$ (Ohishi et al. 1992) for TMC-1. The fractional abundances of C_3H_2 , C_4H and C_4H^- in diffuse clouds in Table 4 were derived from the mean column densities in the last row of Table 3 and scaled to $X(C_2H) = 6 \times 10^{-8}$ (Lucas & Liszt 2000a; Gerin et al. 2011).

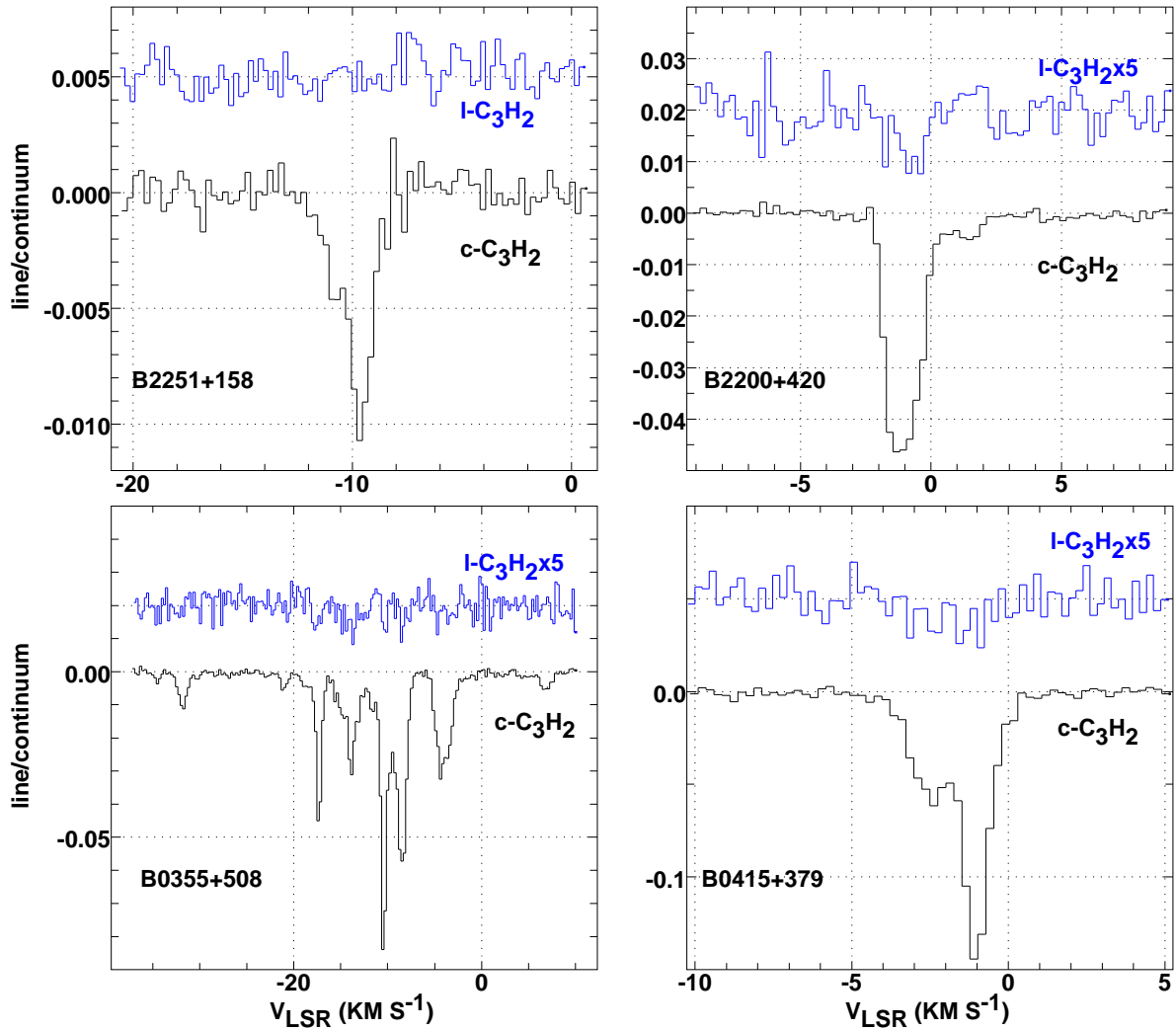


Fig. 1.— Observed absorption line profiles of para linear- and ortho cyclic- C_3H_2 toward four continuum sources. The profiles of l - C_3H_2 have been vertically displaced and scaled as indicated.

3. The abundances of small hydrocarbons in diffuse and dark clouds

Spectra of *c*-C₃H₂ and *l*-C₃H₂ are shown in Fig. 1. From Table 3 we see that $N(l\text{-C}_3\text{H}_2)/N(c\text{-C}_3\text{H}_2) \approx 0.06$ and $N(l\text{-C}_3\text{H}_2)/E_{B-V} \approx 2 \pm 1 \times 10^{11} \text{ (mag.)}^{-1}$. The column densities of *l*-C₃H₂ in local diffuse clouds are some three orders of magnitude smaller than those calculated by Maier et al. (2011b) in order to explain the DIBs (see also Krelowski et al. (2011) and Oka & McCall (2011)).

Beyond the manifest irrelevance of *l*-C₃H₂ to the DIB problem it is possible to make some interesting statements about the abundances of small hydrocarbons in diffuse clouds.

- The ethynyl radical and polyynes (polyynes=C_{*n*}H) C₂H is by far the most abundant of the small polyatomic hydrocarbons, with $N(\text{C}_2\text{H})/E_{B-V} = 7 \pm 2 \times 10^{13} \text{ cm}^{-2}/\text{mag}$. The abundance of C₂H relative to H₂ varies little in diffuse gas with estimates $X(\text{C}_2\text{H}) = 4 - 7 \times 10^{-8}$ (Lucas & Liszt 2000a; Gerin et al. 2011) and $X(\text{C}_2\text{H})$ is nearly the same in diffuse gas and toward TMC-1 (see Table 4). C₂H is no less abundant than CH in diffuse gas (where $X(\text{CH}) = 4 \pm 0.5 \times 10^{-8}$ according to Sheffer et al. (2008) and Weselak et al. (2010)) and is some three times more abundant than CH in TMC-1, see Table 4. Note that this value for $X(\text{C}_2\text{H})$ implies a characteristic value for the molecular hydrogen fraction $f_{\text{H}_2} = 2N(\text{H}_2)/N(\text{H}) = 2N(\text{H}_2)/(N(\text{H I})+2N(\text{H}_2)) \approx 0.4$, given that we measured column densities per unit reddening and $N(\text{C}_2\text{H})/E_{B-V} = (N(\text{C}_2\text{H})/N(\text{H}_2)) \times (N(\text{H}_2)/N(\text{H})) \times (N(\text{H})/E_{B-V})$ with $N(\text{H})/E_{B-V} = 5.8 \times 10^{21} \text{ H cm}^{-2} \text{ mag}^{-1}$ (Bohlin et al. 1978; Rachford et al. 2009). The same value was inferred for the diffuse gas as a whole by Liszt et al. (2010).
- $N(l\text{-C}_3\text{H}_2)/E_{B-V}$ varies by a factor 3, somewhat more than for C₂H or *c*-C₃H₂ (factors < 2 in Table 3) but, as with C₂H, its fractional abundance relative to H₂ is about the same in diffuse gas and toward TMC-1 (Table 4), $X(l\text{-C}_3\text{H}_2) = 2 \times 10^{-10}$. So quite generally one has $X(l\text{-C}_3\text{H}_2)/N(\text{C}_2\text{H}) \approx 1/350$.
- *c*-C₃H₂ and C₂H appear in the fixed proportion $N(c\text{-C}_3\text{H}_2)/N(\text{C}_2\text{H}) = 1/21$ (Lucas & Liszt 2000a; Gerin et al. 2011) in diffuse clouds, implying that $X(c\text{-C}_3\text{H}_2) = 2 - 3 \times 10^{-9}$ with little variation. $X(c\text{-C}_3\text{H}_2)$ is 3-4 times smaller in diffuse clouds compared to TMC-1² and the ratio $N(l\text{-C}_3\text{H}_2)/N(c\text{-C}_3\text{H}_2) = 17$ in diffuse clouds is larger for this reason.
- The column density of C₄H has previously not been strongly-constrained in diffuse clouds (see Lucas & Liszt (2000a)), but C₄H is at most 14% as abundant as C₂H in the two directions for which we have the best limits. The fractional abundance of C₄H in TMC-1

²Fossé et al. (2001) mapped emission from both *l*-C₃H₂ and *c*-C₃H₂ around the position of the polyne peak in TMC-1.

is quite uncertain (Table 4), with estimates ranging between $1 - 9 \times 10^{-8}$ implying $1/6 \lesssim X(\text{C}_4\text{H})/X(\text{C}_2\text{H}) \lesssim 1.5$. All of the C_4H column densities may eventually require re-scaling because the permanent dipole moment of C_4H is uncertain (E. Herbst and S. Yamamoto, private communication).

- The present results represent the first search for C_4H^- in diffuse gas. Despite the high free electron abundance $n(\text{e})/n(\text{H}) \gtrsim n(\text{C}^+)/n(\text{H}) = 1.6 \times 10^{-4}$ (Sofia et al. 2004), the abundance of C_4H^- is very small, $X(\text{C}_4\text{H}^-)/X(\text{C}_2\text{H}) \lesssim 0.001$ or $X(\text{C}_4\text{H}^-) \lesssim 6 \times 10^{-11}$. The abundance of molecular anions is most likely limited in diffuse gas because so much of the ambient hydrogen is in atomic form and anion neutralization by atomic hydrogen is rapid (Eichelberger et al. 2007). Our limits on $N(\text{C}_4\text{H}^-)$ are comparable to those reached by Agúndez et al. (2008) toward TMC-1, which implied $X(\text{C}_4\text{H}^-) < 4 \times 10^{-12}$, but Cordiner (unpublished) recently detected C_4H^- toward TMC-1 with $X(\text{C}_4\text{H}^-) = 1 \pm 0.25 \times 10^{-12}$.

4. Summary and discussion

The sightlines in this work substitute distant radio sources for early-type stars used in optical/uv absorption-line studies, uniquely providing access to a diverse set of polar polyatomic molecules. Nonetheless there are comparable column densities of all species that are accessible in both wavelength regimes, OH, CO and CN (Liszt & Lucas 1996, 1998, 2001) and comparable thermal pressures as judged in the radio by the rotational excitation of CO (Liszt & Lucas 1998). CO column densities are small and the gas-phase carbon is inferred to reside overwhelmingly in C^+ even when $N(\text{C}^+)$ is not measured directly, implying that the ionization fraction is similar even if the flux of ionizing photons will occasionally be larger in optical absorption line studies. Although there is no theory that reliably predicts the abundances of polyatomic molecules in diffuse clouds, similar circumstances should affect both *l*- C_3H_2 and DIBs no matter which measurement technique is employed

The simple hydrocarbons observed and discussed here generally have well-defined abundances with respect to reddening and H_2 over a wide range of conditions, especially CH, C_2H and *c*- C_3H_2 , with slightly larger variations for *l*- C_3H_2 . Bulk effects naturally introduce some degree of superficial correlation with $E_{\text{B}-\text{V}}$ even for unrelated species that are mixed into the ISM along the line of sight, but proportionality between the column densities of small hydrocarbons and $N(\text{H}_2)$ reflects a concentration within regions of high molecular fraction, typically $f_{\text{H}_2} \approx 0.4$ as noted above. This may make the small hydrocarbons rather poorly suited to be candidate carriers for the most heavily-studied DIBs (Friedman et al. 2011; Vos et al. 2011), which do not have obvious associations with $N(\text{H}_2)$ and are more usually attributed to regions of low molecular fraction.

In any case, the column density per unit reddening of $l\text{-C}_3\text{H}_2$ in diffuse clouds is a factor 2000 below the value $N(l\text{-C}_3\text{H}_2)/E_{B-V} = 4 \times 10^{14} \text{ cm}^{-2} \text{ mag}^{-1}$ that was hypothesized by Maier et al. (2011a) in order that $l\text{-C}_3\text{H}_2$ could be the carrier of the DIBs at 4881Å and 5450Å. The most abundant hydrocarbons in diffuse gas, as toward TMC-1, are CH and C_2H with $X(\text{CH}) = 4 \times 10^{-8}$ and $X(\text{C}_2\text{H}) = 6 \times 10^{-8}$. Taken relative to C_2H in diffuse gas one has $X(c\text{-C}_3\text{H}_2)/X(\text{C}_2\text{H}) = 1/21$ and $X(l\text{-C}_3\text{H}_2)/X(\text{C}_2\text{H}) = 1/350$ from the mean values given in Table 3, with $X(\text{C}_4\text{H})/X(\text{C}_2\text{H}) < 1/7$ in the two best cases and $X(\text{C}_4\text{H}^-)/X(\text{C}_2\text{H}) \lesssim 1/1000$ quite generally.

Gredel et al. (2011) review the history of (failed) DIB attributions, including $l\text{-C}_3\text{H}_2$ and the equally recent example of $\text{H-C}_4\text{H-H}^+$, proposed by Krełowski et al. (2010) and criticized by Maier et al. (2011a). Other attributions recently deemed to be insupportable include heavier species such as the simplest PAH naphthalene (C_{10}H_8), anthracene ($\text{C}_{14}\text{H}_{10}$) and their cations (Galazutdinov et al. 2011). Perhaps still hanging in the balance, but by no means generally accepted, is a tentative attribution to CH_2CN^- by Cordiner & Sarre (2007).

Species as complicated as naphthalene are likely to prove as elusive at radio wavelengths as in the optical/uv domain, but the sort of work performed here may be straightforwardly extended to other polar species such as C_3H and CH_2CN , especially considering the modest observing times required and the increasing availability of wider instantaneous bandwidths at the GBT and VLA. Searches may also be possible for non-polar species that are observable in their magnetic dipole transitions as recently discussed by Morse & Maier (2011).

The National Radio Astronomy Observatory is operated by Associated Universities, Inc. under a contract with the National Science Foundation. HL and MG were partially funded by the grant ANR-09-BLAN-0231-01 from the French *Agence Nationale de la Recherche* as part of the SCHISM project (<http://schism.ens.fr/>). MAC acknowledges support from the NASA Astrobiology Institute through the Goddard Center for Astrobiology.

Facilities: Jansky VLA

REFERENCES

- Agúndez, M., Cernicharo, J., Guélin, M., Gerin, M., McCarthy, M. C., & Thaddeus, P. 2008, *A&A*, 478, L19
- Bohlin, R. C., Savage, B. D., & Drake, J. F. 1978, *ApJ*, 224, 132
- Cernicharo, J., Cox, P., Fossé, D., & Güsten, R. 1999, *A&A*, 351, 341

- Cernicharo, J., Gottlieb, C. A., Guelin, M., Killian, T. C., Paubert, G., Thaddeus, P., & Vrtillek, J. M. 1991, *ApJ*, 368, L39
- Cordiner, M. A. & Sarre, P. J. 2007, *A&A*, 472, 537
- Cox, P., Güsten, R., & Henkel, C. 1988, *A&A*, 206, 108
- Cox, P., Walmsley, C. M., & Guesten, R. 1989, *A&A*, 209, 382
- Eichelberger, B., Snow, T. P., Barckholtz, C., & Bierbaum, V. M. 2007, *ApJ*, 667, 1283
- Fossé, D., Cernicharo, J., Gerin, M., & Cox, P. 2001, *ApJ*, 552, 168
- Friedman, S. D., York, D. G., McCall, B. J., Dahlstrom, J., Sonnentrucker, P., Welty, D. E., Drosback, M. M., Hobbs, L. M., Rachford, B. L., & Snow, T. P. 2011, *ApJ*, 727, 33
- Galazutdinov, G., Lee, B.-C., Song, I.-O., Kazmierczak, M., & Krełowski, J. 2011, *Mon. Not. R. Astron. Soc.*, 412, 1259
- Gerin, M., Kaźmierczak, M., Jastrzebska, M., Falgarone, E., Hily-Blant, P., Godard, B., & de Luca, M. 2011, *A&A*, 525, A116
- Gredel, R., Carpentier, Y., Rouillé, G., Steglich, M., Huisken, F., & Henning, T. 2011, *A&A*, 530, A26
- Krełowski, J., Beletsky, Y., Galazutdinov, G. A., Kołos, R., Gronowski, M., & LoCurto, G. 2010, *ApJ*, 714, L64
- Krełowski, J., Galazutdinov, G., & Kołos, R. 2011, *ApJ*, 735, 124
- Liszt, H. & Lucas, R. 2001, *A&A*, 370, 576
- Liszt, H. S. & Lucas, R. 1996, *A&A*, 314, 917
- . 1998, *A&A*, 339, 561
- Liszt, H. S., Pety, J., & Lucas, R. 2010, *A&A*, 518, A45
- Lucas, R. & Liszt, H. S. 2000a, *A&A*, 358, 1069
- . 2000b, *A&A*, 355, 327
- Madden, S. C., Irvine, W. M., Swade, D. A., Matthews, H. E., & Friberg, P. 1989, *Astron. J.*, 97, 1403

- Maier, J. P., Chakrabarty, S., Mazzotti, F. J., Rice, C. A., Dietsche, R., Walker, G. A. H., & Bohlender, D. A. 2011a, *ApJ*, 729, L20
- Maier, J. P., Walker, G. A. H., Bohlender, D. A., Mazzotti, F. J., Raghunandan, R., Fulara, J., Garkusha, I., & Nagy, A. 2011b, *ApJ*, 726, 41
- Matthews, H. E. & Irvine, W. M. 1985, *ApJ*, 298, L61
- Morse, M. D. & Maier, J. P. 2011, *ApJ*, 732, 103
- Ohishi, M., Irvine, W., & Kaifu, N. 1992, in *Astrochemistry of cosmic phenomena: proceedings of the 150th Symposium of the International Astronomical Union, held at Campos do Jordao, Sao Paulo, Brazil, August 5-9, 1991*. Dordrecht: Kluwer, ed. P. D. Singh, 171–172
- Oka, T. & McCall, B. J. 2011, *Science*, 331, 293
- Pety, J., Teyssier, D., Fossé, D., Gerin, M., Roueff, E., Abergel, A., Habart, E., & Cernicharo, J. 2005, *A&A*, 435, 885
- Rachford, B. L., Snow, T. P., Destree, J. D., Ross, T. L., Ferlet, R., Friedman, S. D., Gry, C., Jenkins, E. B., Morton, D. C., Savage, B. D., Shull, J. M., Sonnentrucker, P., Tumlinson, J., Vidal-Madjar, A., Welty, D. E., & York, D. G. 2009, *Astrophys. J., Suppl. Ser.*, 180, 125
- Sakai, N., Saruwatari, O., Sakai, T., Takano, S., & Yamamoto, S. 2010, *A&A*, 512, A31+
- Schlegel, D. J., Finkbeiner, D. P., & Davis, M. 1998, *ApJ*, 500, 525
- Sheffer, Y., Rogers, M., Federman, S. R., Abel, N. P., Gredel, R., Lambert, D. L., & Shaw, G. 2008, *ApJ*, 687, 1075
- Smith, I. W. M., Herbst, E., & Chang, Q. 2004, *Mon. Not. R. Astron. Soc.*, 350, 323
- Sofia, U. J., Lauroesch, J. T., Meyer, D. M., & Cartledge, S. I. B. 2004, *ApJ*, 605, 272
- Thaddeus, P., Vrtilik, J. M., & Gottlieb, C. A. 1985, *ApJ*, 299, L63
- Turner, B. E., Herbst, E., & Terzieva, R. 2000, *Astrophys. J., Suppl. Ser.*, 126, 427
- Vos, D. A. I., Cox, N. L. J., Kaper, L., Spaans, M., & Ehrenfreund, P. 2011, *A&A*, 533, A129
- Weselak, T., Galazutdinov, G. A., Beletsky, Y., & Krełowski, J. 2010, *Mon. Not. R. Astron. Soc.*, 402, 1991

Table 1: Species and transitions observed and column density-optical depth conversion factors

Species	ortho/para	transition	frequency MHz	$\log(A_{kj} \text{ s}^{-1})^a$	$N(X)/\int \tau dv^b$ $\text{cm}^{-2} (\text{km s}^{-1})^{-1}$
C ₄ H ⁻		2-1	18619.76	-5.938	5.41×10^{12}
C ₄ H		N=2-1 J=5/2-3/2 F=2-1	19014.72	-7.671	1.14×10^{15}
C ₄ H		N=2-1 J=5/2-3/2 F=3-2	19015.14	-7.616	7.12×10^{14}
<i>c</i> -C ₃ H ₂	o	1 ₁₀ -1 ₀₁	18343.14	-6.374	1.35×10^{13}
<i>l</i> -C ₃ H ₂	p	1 ₀₁ -0 ₀₀	20792.59	-6.232	9.00×10^{12}

^a www.splatalogue.net

^b for the observed ortho or para version only, assuming rotational excitation in equilibrium with the cosmic microwave background

Table 2: Continuum target, line of sight and line profile properties

Target	l o	b o	E _{B-v} ^a mag	flux ^b %	EW(<i>o-c</i> -C ₃ H ₂) ^c m s ⁻¹	EW(<i>p-l</i> -C ₃ H ₂) m s ⁻¹	EW(C ₄ H) ^d m s ⁻¹	EW(C ₄ H ⁻) m s ⁻¹
B0355+508	150.38	-1.60	1.50	34	320±2	4.0±1.4	<16.8 ^e	<13.3
B0415+379	161.67	-8.82	1.65	9	250±3	7.8±1.8	<40.2	< 11.6
B2200+420	92.59	-10.44	0.33	18	84±1	2.8±0.7	<7.40	< 6.2
B2251+158	86.11	-38.18	0.11	51	170±1	< 2.4	<4.8	< 4.6

^afrom Schlegel et al. (1998)

^b relative to 3C84 (S_v ≈ 16 Jy)

^c EW = $\int \tau dv$ for the observed transition, for C₄H applicable to either transition observed

^e all upper limits are 3σ

Table 3: Total molecular column densities per unit reddening^a

Target	<i>c</i> -C ₃ H ₂ ^b	<i>l</i> -C ₃ H ₂ ^c	C ₄ H	C ₄ H ⁻	C ₂ H ^d	<i>c</i> -C ₃ H ₂ ^d
B0355	38.5±0.20	0.96±0.34	< 66E ^e	< 0.48	607	41.4
B0415	28.2±0.30	1.76±0.39	< 150	< 0.39	519	25.9
B2200	45.7±0.48	3.05±0.76	< 130	< 1.00	939	43.5
B2251	21.1±1.45	< 7.60	< 260	< 2.32	613	
Mean	33±11	1.9±1.1			670±180	

^a Units are 10¹¹ cm⁻² mag⁻¹.

^b N(*c*-C₃H₂) = (4/3) × N(*o-c*-C₃H₂)

^c N(*l*-C₃H₂) = 4 × N(*p-l*-C₃H₂)

^d N(C₂H) and N(*l*-C₃H₂) from Lucas & Liszt (2000b)

^e all upper limits are 3σ

Table 4: Fractional molecular abundances in diffuse clouds^a and TMC-1^{a,b}

Target	X(<i>c</i> -C ₃ H ₂)	X(<i>l</i> -C ₃ H ₂)	X(C ₄ H)	X(C ₄ H ⁻)	X(C ₂ H)	X(CH)
Diffuse	3	0.2	<8 ^{c,d}	<0.07 ^{c,e}	60	40
TMC-1	10 ^{f,g}	0.3 ^h	20 ^{f,i}	0.001 ^j	60 ^{f,k}	20 ^{f,g}

^a In units of 10⁻⁹. Results from Table 3 and X(CH) from Sheffer et al. (2008) and Weselak et al. (2010)

^b N(H₂) = 10²² for TMC-1 (Ohishi et al. 1992)

^c all upper limits are 3σ

^d X(C₄H)/X(C₂H) < 0.14 for B0355 and B2200

^e X(C₄H⁻)/X(C₂H) < 0.0011 for B0355, B0415 and B2200

^f Ohishi et al. (1992)

^g Smith et al. (2004); Turner et al. (2000)

^h Cernicharo et al. (1991), 4E-10 from Turner et al. (2000).

ⁱ 10 × 10⁻⁹ from Turner et al. (2000); 70 × 10⁻⁹ from Agúndez et al. (2008); 90 × 10⁻⁹ from Smith et al. (2004)

^j Cordiner (2012) unpublished. Agúndez et al. (2008) gave X(C₄H⁻) < 0.004 × 10⁻⁹

^k Sakai et al. (2010). Smith et al. (2004) and Turner et al. (2000) give 2E-8